Directionality and Crest Length Statistics of Steep Waves in Open Ocean Waters

NICHOLAS SCOTT AND TETSU HARA

Graduate School of Oceanography, University of Rhode Island, Narragansett, Rhode Island

PAUL A. HWANG

Oceanography Division, Naval Research Laboratory, Stennis Space Center, Mississippi

EDWARD J. WALSH

Observational Science Branch, NASA Goddard Laboratory for Hydrospheric Processes, Wallops Island, Virginia

(Manuscript received 5 January 2004, in final form 30 July 2004)

ABSTRACT

A new wavelet analysis methodology is applied to open ocean wave height data from the Southern Ocean Waves Experiment (1992) and from a field experiment conducted at Duck, North Carolina, in 1997 with the aim of estimating the directionality and crest lengths of steep waves. The crest directionality statistic shows that most of the steep wave crests are normal to the direction of the mean wind. This is inconsistent with the Fourier wavenumber spectrum that shows a broad bimodal directional spreading at high wavenumbers. The crest length statistics demonstrate that the wave field is dominated by short-crested waves with small crest length/wavelength ratios. The one-dimensional steep wave statistic obtained from the integration of the directional (two dimensional) steep wave statistic is consistent with the one-dimensional steep wave statistic obtained from the one-dimensional analysis at high wave slope thresholds.

1. Introduction

The directionality of ocean surface wave fields is of interest for many reasons. Some measurements of the sea surface topography (Hwang et al. 2000) have revealed a bimodal directional distribution in the two-dimensional (2D) wavenumber spectrum, which is in contrast to the unimodal form proposed by many earlier models. The bimodal directional distribution has, in fact, been shown to yield mean square slope values that are more consistent with field studies than the traditional unimodal directional distributions (Hwang and Wang 2001). In addition, the observed bimodal directional spreading is consistent with the theoretical estimate of nonlinear wave interactions, which moves energy away from the peak frequency and redistributes it into the directions oblique to the mean wind direction (Wang and Hwang 2001). Directional spreading is also important in determining the form of the one-dimensional spectrum (Banner 1990).

Corresponding author address: Dr. Nicholas Scott, Applied Ocean Physics and Engineering, Woods Hole Oceanographic Institution, Mail Stop 12, 266 Woods Hole Road, Woods Hole, MA 02543.
E-mail: nscott@whoi.edu

There have been very few studies of directional properties of steep and breaking waves. Recently, Melville and Matusov (2002) obtained images of oceanic whitecaps from an aircraft and tracked the evolution of whitecaps using image velocimetry. They were able to calculate the directional breaking wave statistic $\Lambda(c)$ and found a symmetrical angular distribution about the mean downwind direction.

The traditional methods of understanding the directionality of the wave field have been through the use of Fourier-based methods such as the maximum likelihood method (Capon 1969) and the direct two-dimensional Fourier transform. New methods have recently emerged that take into account the wave groupiness of the ocean surface. Donelan et al. (1996) were able to calculate the frequency–directional spectrum by estimating the instantaneous wave propagation directions at various frequencies using a wavelet-based analysis. However, there have been no observational studies of the directionality of steep nonlinear waves. In addition, there has been no study of the statistical nature of crest lengths on the ocean surface.

Recently, direct observations of ocean surface topography were made during the Southern Ocean Waves Experiment (SOWEX) and an experiment conducted off Duck, North Carolina, in September 1997 (hereafter

termed the DNC experiment). Using these datasets we have developed a data analysis technique to estimate the statistics of nonlinear wave groups based on the wavelet transform. In a companion paper (Scott et al. 2005), we have presented one-dimensional analyses of the steep wave statistics based on the assumption that all steep wave fronts propagate in the mean wind direction. In this paper, we investigate the directionality and crest length statistics of steep wave events in detail by performing two-dimensional analyses of the ocean surface topography.

2. Data analysis

The analysis in this paper was performed on data from the Southern Ocean Waves Experiment and data obtained from a field experiment conducted near Duck, North Carolina, in September 1997. Information on these experiments can be found in Banner et al. (1999) and Hwang et al. (2000). Since the definition of the steep wave statistic based on the wavelet transform is identical to that in the companion paper (Scott et al. 2005), only a brief summary is given below.

a. Definition of the steep wave statistic

The steep wave statistic is defined based on the formulation of the breaking wave statistic $\Lambda(\mathbf{c})$ proposed by Phillips (1985). Using this same idea, the steep wave statistic $\Lambda_T(k, \theta)$ is defined as the total length of steep wave fronts whose wave slope exceeds a set threshold T per unit surface area per unit wavenumber, where an area element in the wavenumber domain is $dk\ k\ d\theta$. Thus,

$$\Lambda_T(k,\theta)dk\ k\ d\theta = \frac{L}{\tilde{A}}, \tag{1}$$

where $\tilde{A}$ is the area of ocean surface, and L is the total length of breaking wave fronts with wavenumbers in the area element $dk\ k\ d\theta$ in the wavenumber domain. The one-dimensional lambda function $\Lambda_T(k)$ is obtained from the integration of $\Lambda_T(k, \theta)$:

$$\Lambda_T(k) = \int \Lambda_T(k, \theta)k\ d\theta. \tag{2}$$

In general, the slope of an individual wave cannot be determined uniquely for random seas with a broad-banded spectrum. Thus the wave slope is defined using the wavelet transform such that the estimated slope of a steep wave event is, in fact, the average wave slope of a small group of waves that are detected by the wavelet transform.

b. Wavelet transform

The wavelet transform of a signal $f(u)$ in this study is defined as

$$Wf(a, s) = \mathrm{Re}\left[\int_{-\infty}^{\infty} f(u)\frac{1}{a^2}\Psi\left(\frac{u-s}{a}\right)du\right] a > 0, \tag{3}$$

where

$$\Psi(a, s) = \Psi(s/a) = e^{-iK_0 s/a}e^{-1/2\,(s/a)^2},\ K_0 = 5 \tag{4}$$

is the Morlet wavelet. A signal with a high wave slope event at scale a_0 and position s_0 will have a wavelet transform characterized by a large peak value of Wf at (a_0, s_0). The peak value is proportional to the average wave slope in the neighborhood of s_0.

c. Estimation of the two-dimensional steep wave statistic, Λ_T(k, θ)

The observed wave topography data are preprocessed such that the surface elevation is defined at equally spaced grid points both in the along-wind direction and in the cross-wind direction. The wavelet transform is applied to each column vector (in the along-wind direction) of the two-dimensional surface elevation array. The result $Wf(a, s)$ contains an array of high wave slope events. To obtain a distribution of these events, a wave slope threshold is applied over it. All points with a wavelet transform value above a set wave slope threshold T are selected. These points appear as aggregates in local regions of $Wf(a, s)$. From these groups of points, the point of highest value is sought using a nine-point box filter. The local maximum that satisfies the condition of being above the set wave slope threshold is defined as a steep wave crest associated with a wave group. The conversion of the scale a used in the wavelet analysis to the real wavenumber scale k is obtained via a conversion constant, C, such that $k = C/a$. The wavenumber associated with the Morlet wavelet at scale a is taken to be the wavenumber at the peak of its Fourier power spectrum.

The wavelet transform threshold used to discriminate high wave slope events corresponds to a real average wave slope threshold. The conversion from the wavelet transform peak value to the real wave slope threshold is accomplished by first taking a pure sinusoid, $f(u) = A\sin ku$, of known wave amplitude A and wavenumber k and obtaining the wavelet transform of the signal. The peak value of the wavelet transform is then related to the wave slope Ak to determine the conversion constant γ:

$$\gamma = \frac{Ak}{\max[Wf(a, s)]}. \tag{5}$$

With real surface wave height data, this constant is used to convert from the local maximum value of the wavelet transform to the equivalent local wave slope threshold.

The two-dimensional steep wave statistic $\Lambda_T\ (k, \theta)$ can be estimated by first applying the wavelet transform to all along-wind column vectors of the two-

dimensional surface elevation array. The results of the wavelet analysis of a single surface elevation image from the DNC dataset are shown in Figs. 1a and 1b for the wave slope thresholds of 0.02 and 0.06, respectively. Notice that there are no high slope events near the edge of the wave image since we cannot use the wavelet transform data near the edge of the wave height record (Scott et al. 2005). All steep wave events are indicated by circles, and the circle size is proportional to the wave scale (i.e., inverse of the wavenumber). There is a tendency for high wave slope events of the same scale or nearly the same scale to be positioned close to one another. These local events of a common scale together form crests of different lengths distributed over the entire surface elevation image. To study the statistics of crest angle and length, and for the sake of simplicity, we postulate that, to the first order, the high wave slope wave crests form geometrically straight lines on the ocean surface. First, each high wave slope event is classified according to its scale into one of the set discrete scale bins. The scale bins are defined with a set interval of log$a$ or log$k$. Initially, we choose this interval to be 0.1; that is, the wave scale of roughly $\pm 10\%$ is put in the same scale bin.

The second aspect of grouping is carried out by taking high wave slope events of the same scale bin that are positioned less than one pixel away in the along-wind or cross-wind direction as part of a complete wave crest. This is done to simulate, as closely as possible, the continuity of wave crests across the ocean surface. A straight line is drawn from the first high wave slope event to the last high wave slope event that forms a

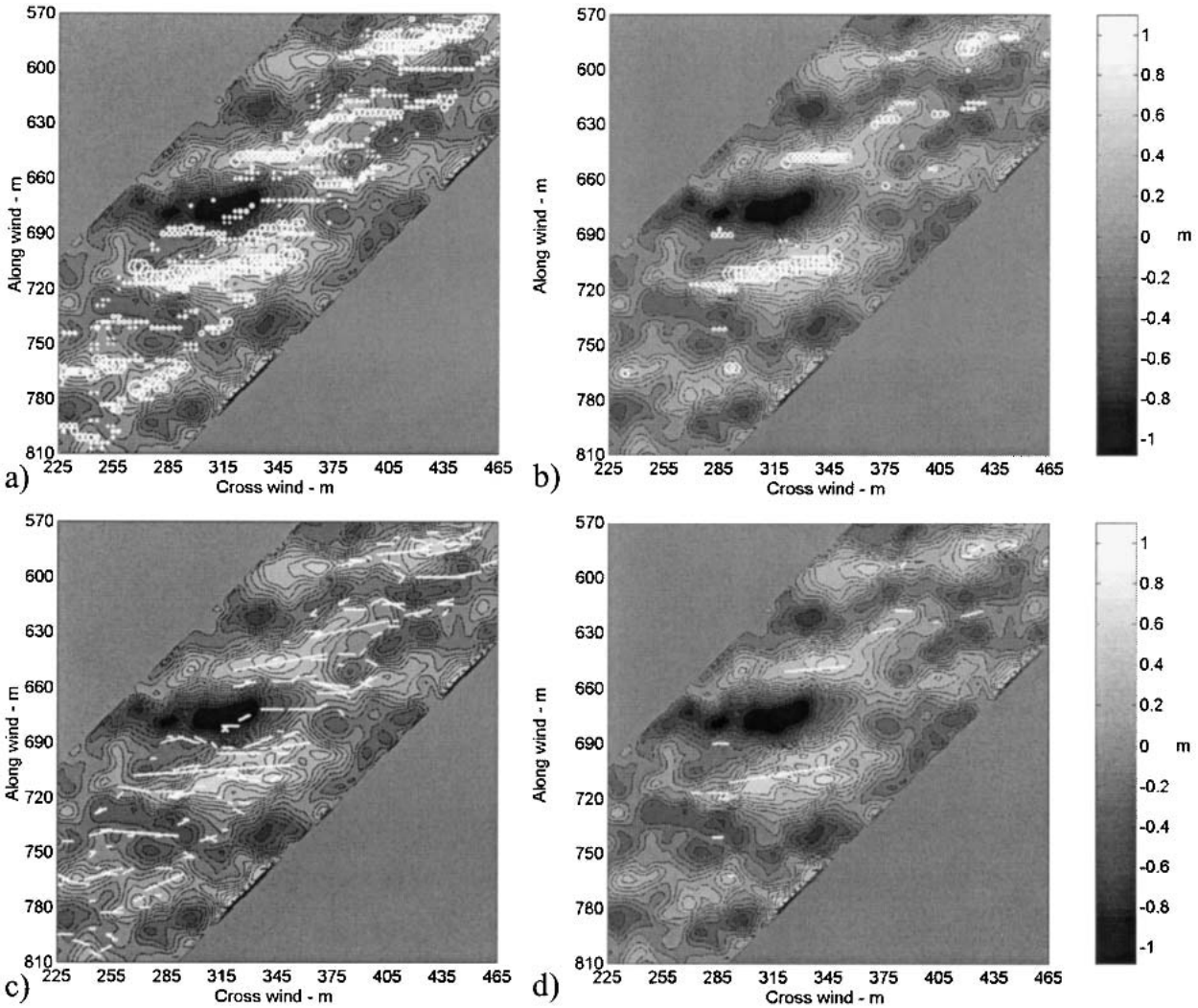

FIG. 1. Contour plot of surface wave topography and high wave slope crests for DNC experiment. Mean wind speed is 9.5 m s^{-1}. (a) Circles indicate crest locations, circle size is proportional to inverse of wavenumber, and wave slope threshold is 0.02. (b) Same as in (a) but wave slope threshold is 0.06. (c) Lines indicate wave crests, and wave slope threshold = 0.02. (d) As in (c) but wave slope threshold is 0.06.

complete wave crest of a common wave scale bin. Figures 1c and 1d show all wave crests defined in this manner in Figs. 1a and 1b, respectively. The length of each line, which is a measure of the length of the crest, is calculated using the equation,

$$d = \sqrt{[(y_2 - y_1) \times \Delta y]^2 + [(x_2 - x_1) \times \Delta x]^2}, \quad (6)$$

where (x_1,y_1) and (x_2,y_2) are the coordinates of the beginning and end positions of the high wave slope crest, and Δy and Δx are along-wind and cross-wind sampling intervals, respectively.

The high wave slope crests in wave groups are positioned at different angles with respect to the wind direction. Thus, the assigned scale, based on the along-wind wavelet transform, is not necessarily the true scale of the high wave slope event. The assigned scale has been determined based on the high slope event measured along the wind direction, while the true scale should be determined based on the event measured perpendicularly to the wave crest. Thus, the true scale $\tilde{a}$ of an event is dependent on the angle of the high wave slope crest and is estimated as

$$\tilde{a} = a \sin(\theta), \quad (7)$$

where θ is the angle that the crest line makes with the wind direction in the clockwise direction, which is calculated according to the following equation:

$$\theta = \tan^{-1}\left[\frac{(x_2 - x_1)\Delta x}{(y_2 - y_1)\Delta y}\right]. \quad (8)$$

It ranges from 0° to 180°, thus making θ devoid of negative values. Any high wave slope wave crests that consist of a single high wave slope event are ignored.

We then estimate $L_T(a, \theta)$, the total length of crests found in the image area as a function of scale and angle. It should be understood from this point on that the scale value a is actually the corrected value $\tilde{a}$. Before the steep wave statistic is calculated, one more correction is needed. Steep wave crests that are not perpendicular to the wind appear less steep than in actuality. Thus the true threshold value $\tilde{T}$ is related to the apparent threshold value T as $\tilde{T} \sin(\theta) = T$, and the appropriate values of $L_T(a, \theta)$ must be redistributed into the higher wave slope threshold distributions. (From this point on the threshold T is actually the corrected value $\tilde{T}$.) Finally, $\Lambda_T(a, \theta)$ is found via the equation

$$\Lambda_T(a, \theta) = \frac{L_T(a, \theta)}{a \times \tilde{A} \times \Delta\theta \times \Delta a}, \quad (9)$$

where $\tilde{A}$ is the total area of the image, $\Delta\theta$ is the differential angle element, and Δa is the differential scale bin element. The steep wave statistic $\Lambda_T(k, \theta)$ is obtained via the equation

$$\Lambda_T(k, \theta) = -\frac{a}{k}\frac{da}{dk}\Lambda_T(a, \theta) = \frac{a^4}{C^2}\Lambda_T(a, \theta). \quad (10)$$

The resulting values of $\Lambda_T(k, \theta)$ are averaged over many datasets to obtain an average two-dimensional steep wave statistic. Integration of the above function over all angles yields the one-dimensional steep wave statistic $\Lambda_{*T}(k)$.

In the companion paper (Scott et al. 2005), the Doppler shift due to the aircraft motion has been corrected for in calculating $\Lambda_T(k)$ by assuming that all waves propagate in the mean wind direction. In this paper, however, we do not attempt to remove the Doppler shift effect from the data because the focus here is on the geometry (directionality and crest length) of steep waves, and the Doppler shift correction complicates such analyses.

d. Estimation of high wave slope crest length distribution $H(d/\lambda)_{\bar{k}}$

In addition to yielding $\Lambda_T(k)$, the wavelet analysis allows for the estimation of the distribution of high wave slope events that possess a particular ratio of crest length to wavelength, d/λ. A two-dimensional distribution $H(d, k)$ is first estimated. This distribution is defined as the number of high wave slope events of wavenumber k and crest length d relative to the total number of high wave slope events. If the distribution $H(d, k)$ is integrated over all d and k, the result is equal to one. There is a one to one relationship between wavenumber k and wavelength λ. Thus, the two-dimensional distribution $H(d, k)$ can be converted to the two-dimensional distribution, $H(d/\lambda, k)$. This can in turn be integrated over set wavenumber intervals. This quantity is denoted by $H(d/\lambda)_{\bar{k}}$, where $\bar{k}$ designates the mean wavenumber of the wavenumber interval used. For the DNC experiment, $H(d/\lambda, k)$ was integrated over $0.05 < k < 0.25$ rad m^{-1} and $0.25 < k < 0.65$ rad m^{-1}, with the mean wavenumber of $\bar{k} = 0.15$ rad m^{-1} and 0.45 rad m^{-1}, respectively. For the SOWEX experiment, $H(d/\lambda, k)$ was integrated over $0.01 < k < 0.05$ rad m^{-1} and $0.05 < k < 0.11$ rad m^{-1}, with the mean wavenumbers of $\bar{k} = 0.03$ rad m^{-1} and 0.08 rad m^{-1}, respectively.

e. Estimation of the crest directionality $P(\theta)$

In addition to the distribution of the length of crests, the distribution of angles that the high wave slope crests make with the mean wind direction can be estimated. Assuming self-similarity and also in order to reduce statistical scatter, the directional distribution $P(\theta)$ is simply defined as the number of high wave slope events of angle θ relative to the total number of high wave slope events such that, if it is integrated over all θ, the result is equal to one. This method of analysis is used for images from both datasets.

3. Results and discussion

a. Detection of steep wave crests

Figures 1a and 1b display the spatial distribution of high wave slope events and the contours of the surface wave topography at wave slope thresholds of 0.02 and 0.06, respectively, from one image of the DNC dataset. The size of the circles is proportional to the wave scale. Figures 1c and 1d show corresponding crest lines defined by connecting the high wave slope events of similar scales. The results from the SOWEX 10 June dataset are shown in Figs. 2 and 3. In Fig. 1 the wind is blowing in the direction from top to bottom. In Figs. 2 and 3 the wind is blowing from bottom to top. The wavelet analysis algorithm is successful in tracking the high wave slope crests at a specific threshold. The wave field is composed of large waves on top of smaller waves on top of the smallest waves. The plotted topography emphasizes the large-scale features rather than the small scale and, thus, small-scale riding waves cannot be readily seen. The wavelet analysis, however, performs multiscale filtration of the data to reveal steep wave crests at many scales. This is the reason for the appearance of crest lines mostly, but not always, near the local peaks of the background topography. In addition, crest lines are occasionally offset from the actual crest locations because of the convolution associated with the wavelet transform.

b. Comparison of the steep wave statistic from 1D and 2D analyses

In Fig. 4, we present the results of the steep wave statistic $\Lambda_T(k, \theta)$ obtained from the integration of the directional steep wave statistic $\Lambda_T(k, \theta)$ over all angles, for the DNC and SOWEX datasets. They are compared with the steep wave statistic $\Lambda_T(k)$ from the one-dimensional analysis described in the companion paper (Scott et al. 2005) without the Doppler correction. The steep wave statistic resulting from the two-dimensional analysis $\Lambda_{*T}(k)$ is similar in form to $\Lambda_T(k)$ obtained from the one-dimensional analysis. The values of $\Lambda_{*T}(k)$ are slightly larger than those of $\Lambda_T(k)$ at low wave slope thresholds. This is due to the fact that, at the

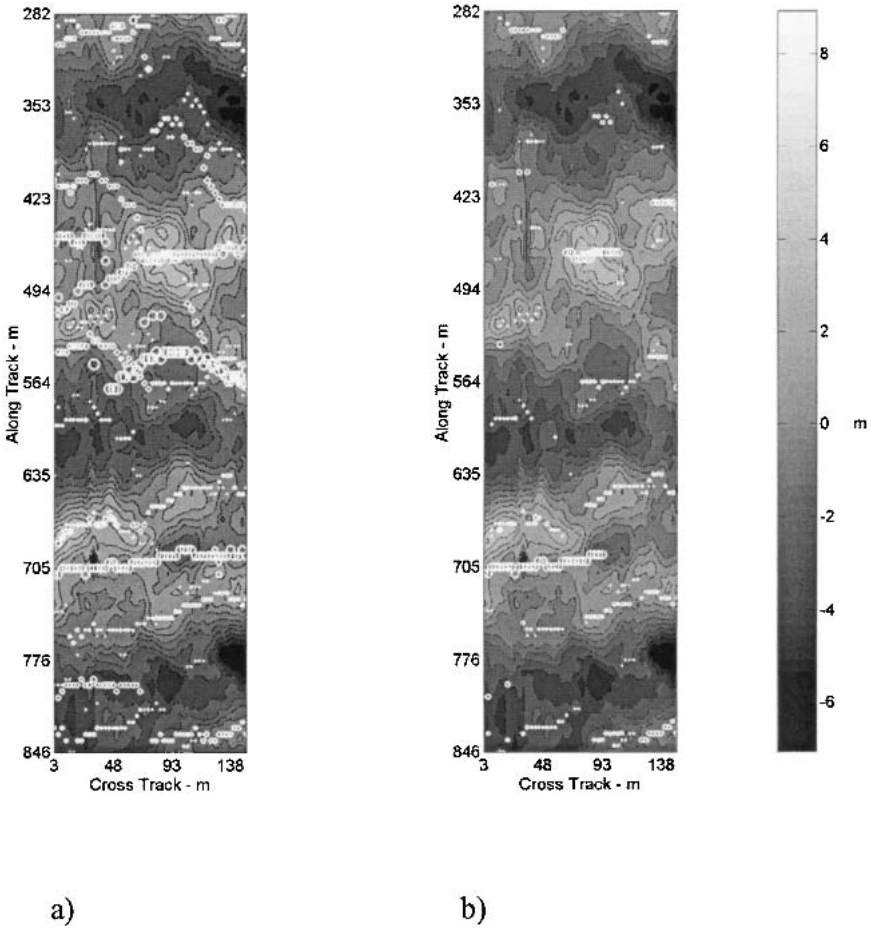

FIG. 2. As in Figs. 1a,b but for 10 Jun SOWEX, and mean wind speed is 25 m s^{-1}.

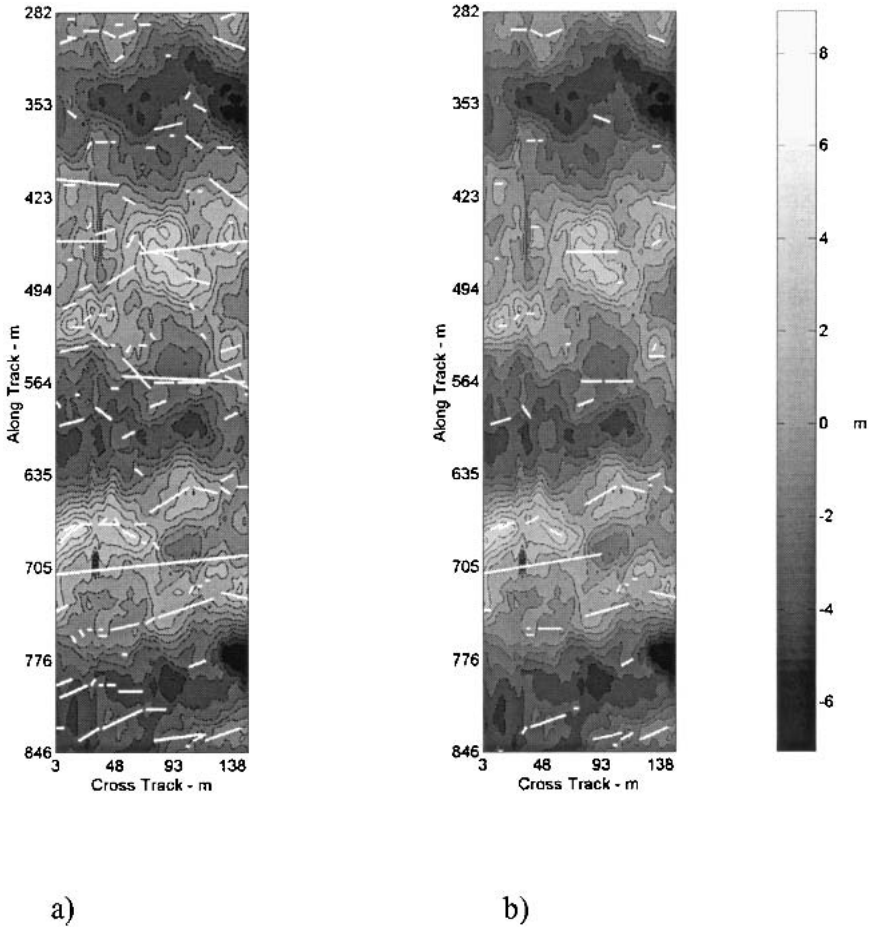

FIG. 3. As in Figs. 1c,d but for 10 Jun SOWEX, and mean wind speed is 25 m s^{-1}.

lower wave slope thresholds, almost all waves are counted. Some wave crests exist at nonnormal angles to the mean wind direction. This causes an increase in the measurement of the total length of wave crests per unit wavenumber per unit area when the two-dimensional analysis is used. The deviation between the two statistics decreases with increasing wave slope threshold, although the signals become quite noisy as the wave slope threshold nears the highest thresholds used in the analysis. Thus, $\Lambda_T(k)$ for both methods of analysis agree reasonably well at the moderately high wave slope threshold regime, implying that most of the steep waves propagate in the direction of the mean wind. This finding justifies the simpler one-dimensional approach taken in our companion paper (Scott et al. 2005).

c. *Directionality of steep wave crests*

Figure 5 displays the statistical distribution $P(\theta)$, the angular distribution of the steep wave crests relative to the wind direction for different wave slope thresholds T. The mean wind is positioned at the angular position of 90°, which is designated by the vertical line. The sequence of figures shows overall that most of the steep waves propagate in the direction of the wind. This gives further affirmation to the assumption made in the companion paper, that is, the assumption of the wave crests predominantly being perpendicular to the direction of the wind. Large-scale ocean surface waves possess curvature and thus in actuality cannot be modeled truly as straight lines. However, most of the steep waves on the ocean surface are small-scale waves whose fronts do not extend considerably over the ocean surface and therefore do not have extensive curvature. Thus, the assumption of the model should not have a large effect on the narrowness of the distribution. The tightness of the distribution $P(\theta)$ about the wind direction demonstrates qualitatively the characteristic of the breaking wave statistical model proposed by Phillips (1985), who predicted the directionality of the breaking wave statistic to be tighter than that of the wavenumber spectrum.

There is a noticeable difference in $P(\theta)$ with changes in wave slope threshold. Each case from both the DNC and the SOWEX datasets shows a growing fraction of

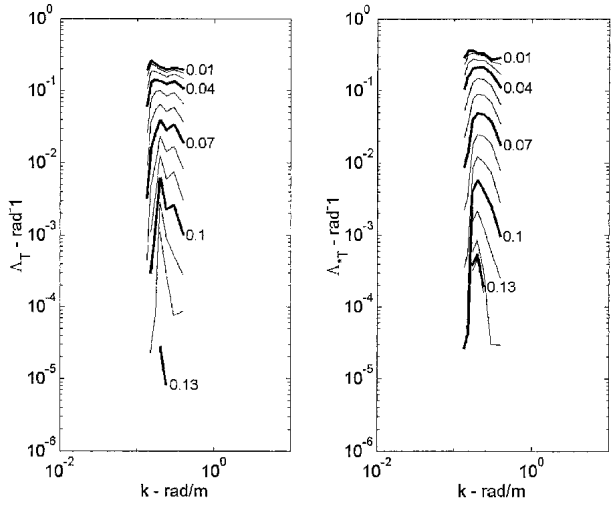

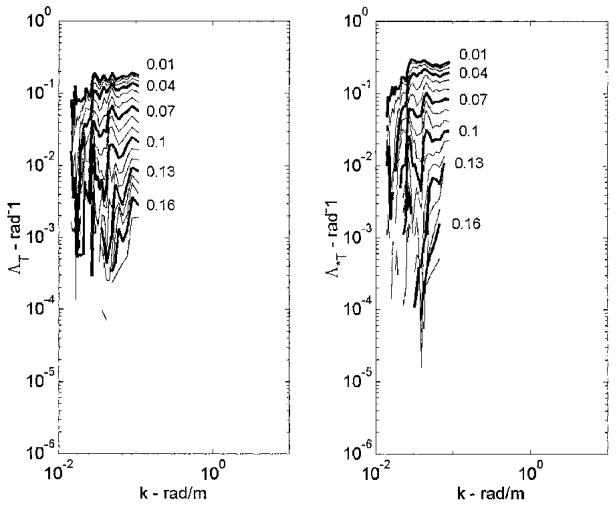

FIG. 4. The steep wave statistics $\Lambda_T(k)$ vs k and $\Lambda_{*T}(k)$ vs k for different wave slope threshold values. Numbers in the figure indicate slope threshold T. (a) DNC experiment and (b) 10 Jun SOWEX.

wave crests propagating in the direction of the mean wind with increases in wave slope threshold. The analysis of the field data by Hwang et al. (2000) from the DNC experiment found a bimodal directionality to the wavenumber spectrum at high wavenumbers above 3 times the peak wavenumber, suggesting that many waves propagate at angles other than downwind. However, the directional spreading of the steep wave statistic is very narrow in Fig. 5. A plausible reason why there is a discrepancy between the wavenumber spectrum and the results of the steep wave statistic is that the Fourier spectrum of short-crested waves causes energy leakage at oblique angles even if the wave crest itself is perpendicular to the wind direction. Since the steep wave analysis is only a quasi-two-dimensional analysis, it does not produce energy leakage at the oblique angles.

d. Crest length statistics

Figure 6 shows the statistical distributions $H(d/\lambda)_{\bar{k}}$ of the ratio between the crest length and the wavelength. The plots show two distributions for the low and high wavenumber bins defined earlier. There is a dearth of data points in the low wavenumber bin but the trends are clear. The distributions show that most of the waves have small crest length/wavelength ratios d/λ. There appears to be self-similarity of the wave shape such that $H(d/\lambda)_{\bar{k}}$ decays with d/λ in a similar manner regardless of the wavenumber and the slope threshold. Thus short-crested waves make more contributions to the total length of wave crests.

4. Sensitivity to wave binning and scale selection

The results of crest directionality and crest length statistics are contingent on how the steep wave events are found and binned to form a continuous wave front on the ocean surface. Initially, each high wave slope event was classified into the scale bins that are defined with a set interval of 0.1 in log$a$ or log$k$. Two other different binning intervals of 0.05 and 0.075 in log$a$ or log$k$ were used to define the wave crests. The results are shown in Fig. 7. The series of figures clearly shows that there is no significant difference due to different scale binning.

5. Conclusions

The wavelet analysis methodology presented here is able to track steep wave events and give estimates of the amount and directionality of high wave slope events that cover a given area of ocean. Analysis of the results shows that high wave slope crests appear over the entire range of wavenumbers resolved and mostly perpendicular to the mean wind direction. Comparison of the steep wave statistic $\Lambda_T(k)$ from the one-dimensional analysis and $\Lambda_{*T}(k)$ obtained by integrating the two-dimensional steep wave statistic shows consistency at moderate wave slope threshold values.

Our crest directionality statistic further confirms that most of the steep wave crests are normal to the direction of the wind even at low wave slope thresholds. This is not consistent with the Fourier wavenumber spectrum that shows a bidirectional spreading at high wavenumbers. The lack of consistency may be partly attributed to the fact that most steep waves are short crested and generate leakage in oblique directions in the Fourier spectrum.

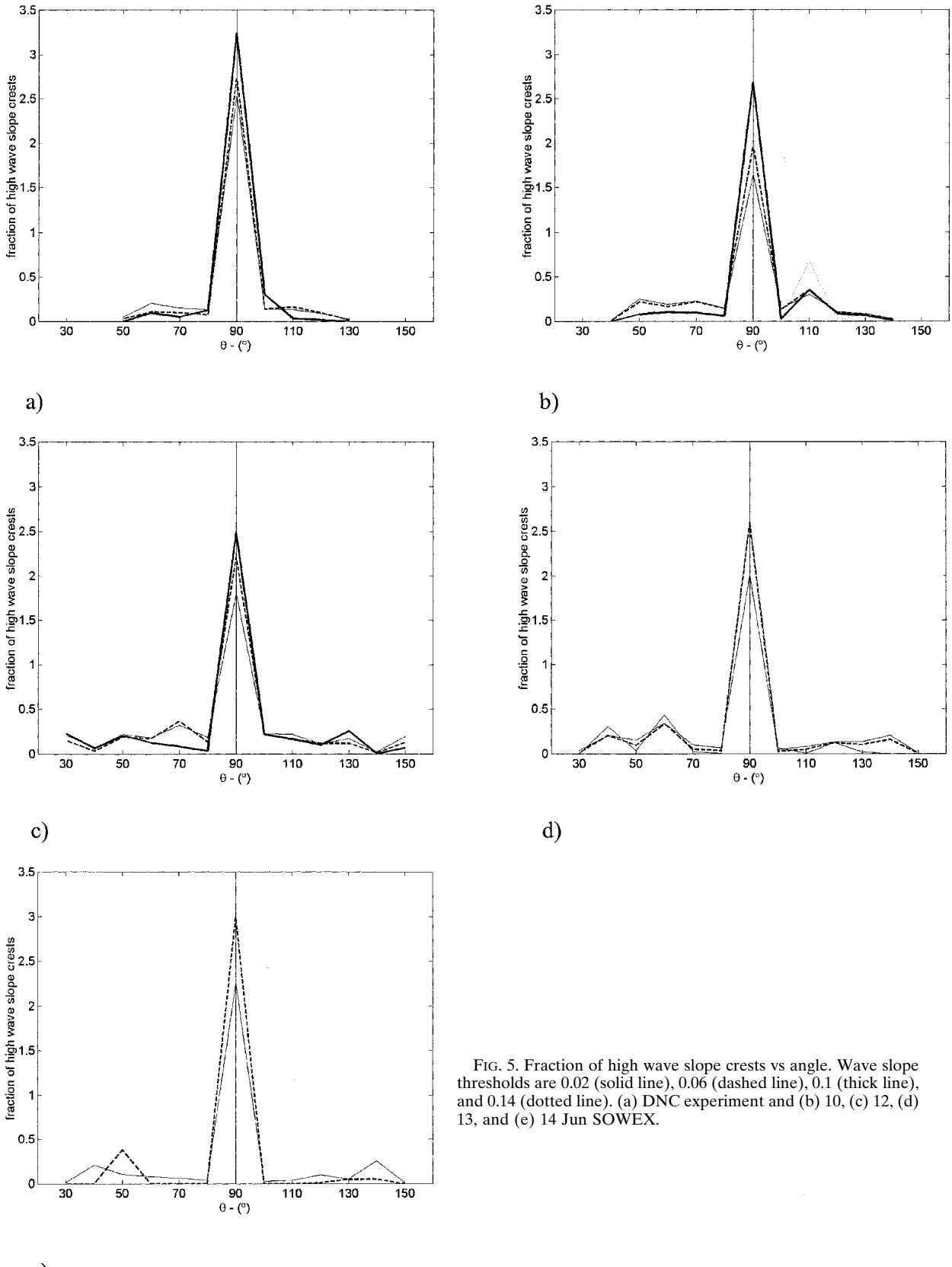

FIG. 5. Fraction of high wave slope crests vs angle. Wave slope thresholds are 0.02 (solid line), 0.06 (dashed line), 0.1 (thick line), and 0.14 (dotted line). (a) DNC experiment and (b) 10, (c) 12, (d) 13, and (e) 14 Jun SOWEX.

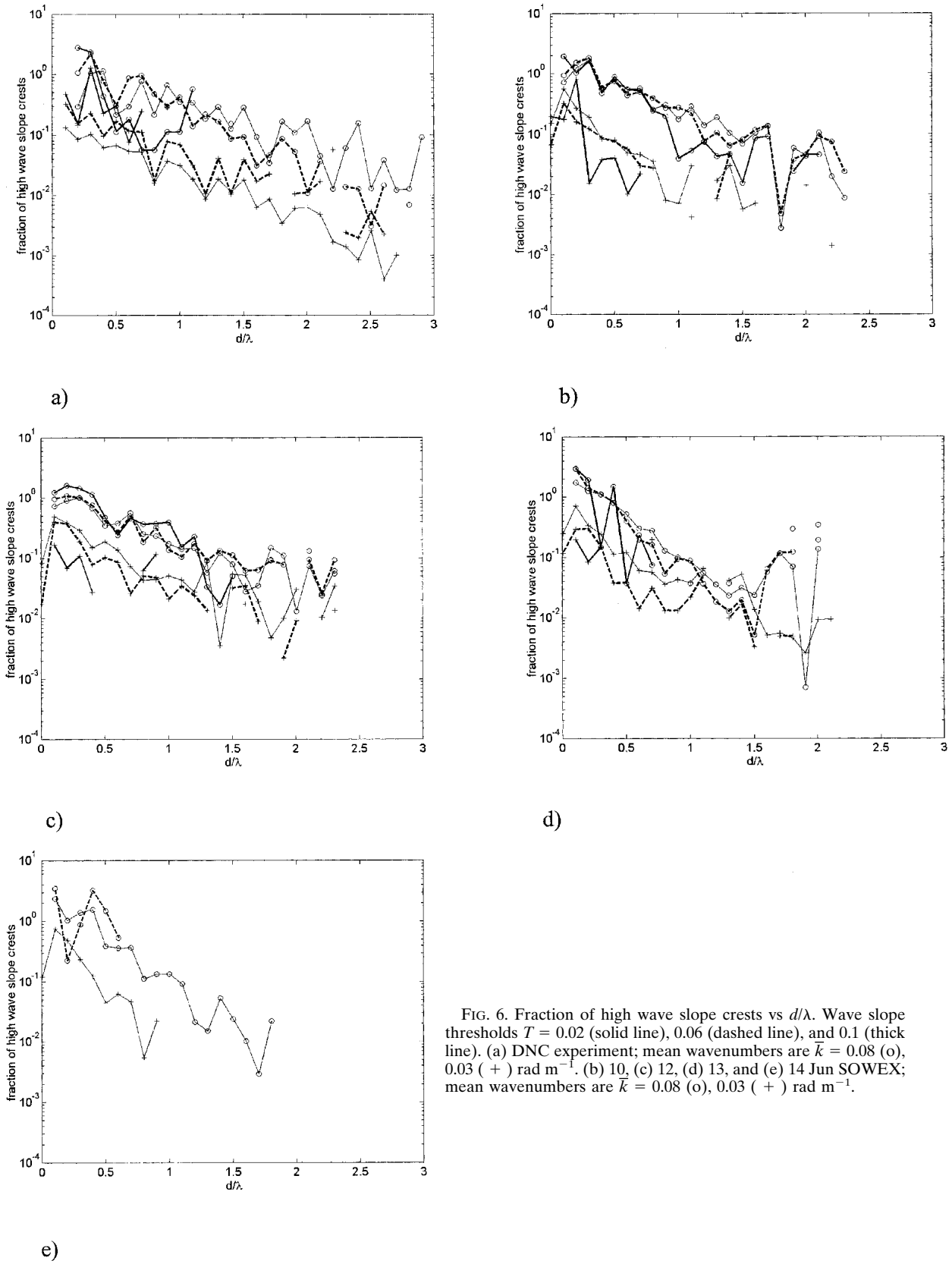

FIG. 6. Fraction of high wave slope crests vs d/λ. Wave slope thresholds $T = 0.02$ (solid line), 0.06 (dashed line), and 0.1 (thick line). (a) DNC experiment; mean wavenumbers are $\bar{k} = 0.08$ (o), 0.03 (+) rad m^{-1}. (b) 10, (c) 12, (d) 13, and (e) 14 Jun SOWEX; mean wavenumbers are $\bar{k} = 0.08$ (o), 0.03 (+) rad m^{-1}.

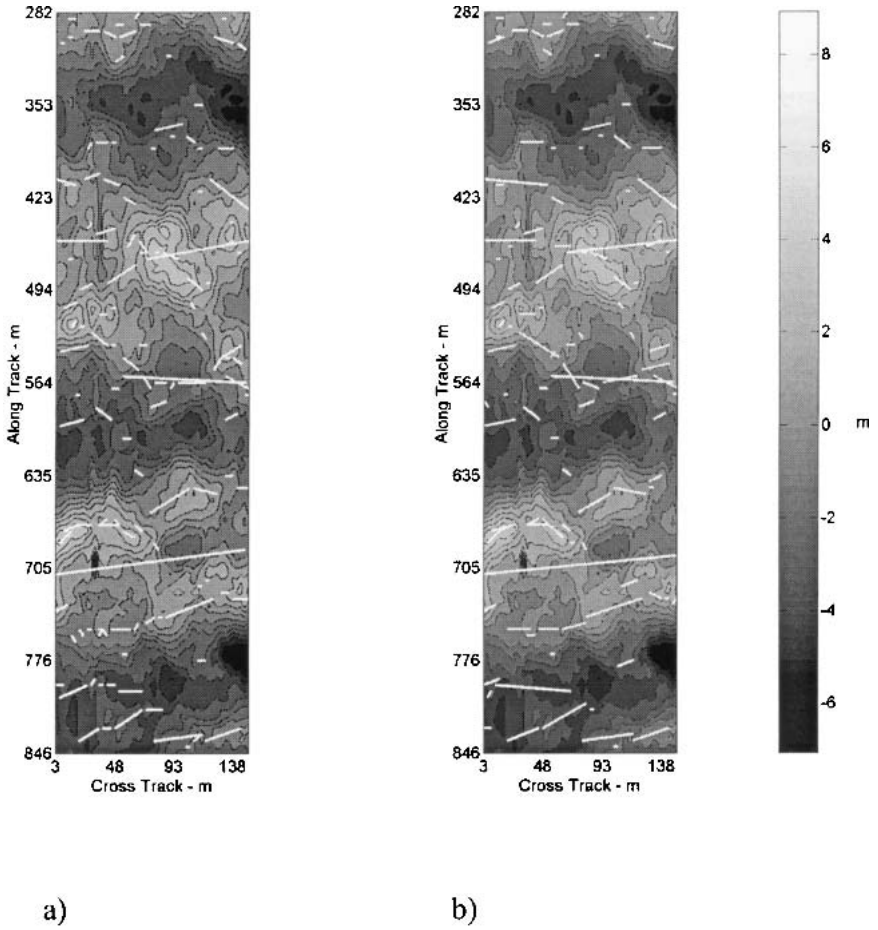

FIG. 7. High wave slope crest lines and contour plot of surface wave topography for 10 Jun SOWEX. Wave slope threshold is 0.02. Mean wind speed is 25 m s^{-1}. (a) Set interval of 0.05 in log*a*, and (b) set interval of 0.075 in log*a*.

Acknowledgments. We acknowledge the helpful comments from Dr. Stephen Belcher, Dr. Michael Banner, and Dr. David Wang. This research was supported by the National Science Foundation Grant OCE0002314. Partial support was also provided from the Naval Research Laboratory under grant N00173021G982 and the Office of Naval Research under grant N00014-0110125.

REFERENCES

Banner, M. L., 1990: Equilibrium spectra of wind waves. *J. Phys. Oceanogr.,* **20,** 966–984.

——, W. Chen, E. J. Walsh, J. B. Jensen, S. Lee, and C. Fandry, 1999: The Southern Ocean Waves Experiment. Part I: Overview and mean results. *J. Phys. Oceanogr.,* **29,** 2130–2145.

Capon, J., 1969: High-resolution frequency–wavenumber spectrum analysis. *Proc. IEEE,* **57,** 1408–1418.

Donelan, M. A., W. M. Drennan, and A. K. Magnusson, 1996: Nonstationary analysis of the directional properties of propagating waves. *J. Phys. Oceanogr.,* **26,** 1901–1914.

Hwang, P. A., and D. W. Wang, 2001: Directional distributions and mean square slopes in the equilibrium and saturation ranges of the wave spectrum. *J. Phys. Oceanogr.,* **31,** 1346–1360.

——, ——, E. J. Walsh, W. B. Krabill, and R. N. Swift, 2000: Airborne measurements of the wavenumber spectra of ocean surface waves. Part I: Spectral slope and dimensionless spectral coefficient. *J. Phys. Oceanogr.,* **30,** 2753–2767.

Melville, W. K., and P. Matusov, 2002: Distribution of breaking waves at the ocean surface. *Nature,* **417,** 58–63.

Phillips, O. M., 1985: Spectral and statistical properties of the equilibrium range in wind-generated gravity waves. *J. Fluid Mech.,* **156,** 505–531.

Scott, N., T. Hara, E. J. Walsh, and P. A. Hwang, 2005: Observations of steep wave statistics in open ocean waters. *J. Atmos. Oceanic Technol.*, **22,** 258–271.

Wang, D. W., and P. A. Hwang, 2001: Evolution of the bimodal directional distribution of ocean waves. *J. Phys. Oceanogr.,* **31,** 1200–1221.